JNCS Journal of Nepal Chemical Society
DOI: https://doi.org/10.3126/ jncs.v45i1.74494
RESEARCH ARTICLE
January 2025, Vol. 45, No. 1, 143-155

In silico Exploration of Potent Phytoecdysteroids Targeting Multiple Receptors in Non-Small Cell Lung Cancer

Bishnu Adhikari[1], Ashish Phuyal[2], Anuraj Phunyal[2], Nabin Upadhyaya[2], Amar Waiba[2], Achyut Adhikari[2*]

[1]*Department of Chemistry, Trichandra Multiple Campus, 44605 Kathmandu, Nepal*

[2]*Central Department of Chemistry, Tribhuvan University, Kirtipur 44618 Kathmandu, Nepal*

[*] Corresponding E-mail: achyutraj05@gmail.com

(Received: December 25, 2024; revised: January 12; 2025 accepted: January 16, 2025)

Abstract

Cancer is a genetic disease that disrupts the normal functioning of cells. This is a disease wherein there is the survival of the old cells that should die while the growth of new and not-needed cells takes place. In this regard, the study has explored virtual screening, molecular docking, and server-based approaches - 10 ns RMSF calculations and prediction of inhibition towards cancer to identify probable candidates from the database of Phytoecdysteroids. Brainesteroside A showed better binding affinities at -9.1 kcal/mol as compared to the reference drug, Gefitinib (-7.0 kcal/mol), and native ligand (-8.5 kcal/mol), for the 7VKO receptor. For the 3ZBF receptor, Ecdysterone22-benzoate 25-O-β-D-glycoside showed better binding affinities, - 9.4 kcal /mol, as compared to the reference drug Gefitinib (-7.0 kcal/mol) and native ligand (-8.4 kcal/mol). Similar binding values with the 3VHK receptor were found in this study, with a better affinity of Polypodine B 2-β-D-glucoside, -9.3 kcal/mol, than either the reference drug (Gefitinib) with values of -7.0 kcal/mol, or native ligand, -9.1 kcal/mol binding values. This study resulted in the promising identification of ROS1, Trka, and VEGFR2 potential inhibitors that showed favorable pharmacokinetic, and pharmacodynamics properties with server-based results. Therefore, this study proposed the use of Phytoecdysteroids as a promising candidate for further lung cancer drug development.

Keywords: ADMET; Molecular Docking; Molecular Dynamics; Binding Affinities.

Introduction

Cancers, which is the main reason for the death of human beings each year in the world [1]. There are many types of cancer based on the specific tissue or organs where abnormal cell growth occurs. Among them, Lung cancer is a type of cancer that develops in the trachea, bronchus, or lung. It can be categorized into two main types: small-cell lung cancer (SCLC) and non-small-cell lung cancer (NSCLC) [2]. NSCLC is the most common, affecting approximately 80% to 85% of lung cancer patients, and with its aggressive nature, rapid spread, and frequent recurrence, a majority of patients are diagnosed at a late stage [3]. Small cell lung cancer (SCLC) comprises 10-15% of lung cancer cases. It has smaller-sized cells that grow and spread rapidly. SCLC usually begins in the bronchi, which is located between the chests. Typically, NSCLC grows and spreads more slowly than SCLC. An NSCLC tumor often has larger-sized cells. NSCLC can be further divided into three subtypes: Squamous-cell carcinoma, adenocarcinoma, and large-cell carcinoma. Adenocarcinoma is the most common form of lung cancer, and it consists of 30% of all lung cancer and 40% of NSCLC [4]. TrkA, ROS1, and VEGFR2 are therapeutic targets in NSCLC and play a crucial role in the cell signaling pathway. Specific drugs for these targets are still lacking. Phytoecdystreoids are a class of

polyhydroxylated compounds that occurs naturally with a structure related to both insect moulting hormone and the plant hormone brassinosteroids. These actions play a critical role in their preventive effects through the induction of programmed cell death [5]. This work tends to identify tyrosine kinase inhibitors from the pool of phytoecdystereoids through ADMET analysis, molecular docking, cancer inhibition prediction, and RMSF of adducts. These results help to identify hit candidates which is useful for the drug development process of lung cancer [6].

Materials and Methods

Ligand Preparation

A total of 382 Phytoecdysteroids were used after a thorough literature review and ChemDraw (https://perkinelmer-chemdraw-professional.software.informer.com/16.0/) to prepare the ligand library for molecular docking calculations. The prepared two-dimensional ligands were saved in. cdx format. All the.cdx files were converted into sdf format by using Open Babel GUI. Avogadro [7] program was used to convert the two-dimensional structure to a three-dimensional structure and energy was minimized using the UFF (Universal Force Field) force field in 2000 steps using a conjugate gradients algorithm. Hydrogen was also added and saved in pdb format from PyMOL v2.5.7 [8]. It was converted to pdbqt format by using AutoDockTools v1.5.7 before molecular docking calculations.

Protein Structure Preparation, Homology modelling, and Validation

By the use of homology modeling, more accurate three-dimensional protein models with known experimental structures were created using the server SWISS MODEL (https://swissmodel.expasy.org/)workspace [9]. To achieve this, the basic local alignment search tool (BLAST) was used to find the homologs that might be used as a template. The templates were chosen to have good resolution, high similarity with the target, and the highest Global Modelling Quality Estimate (GMQE) value [10]. The accuracy of the protein was further verified on the SAVES v6.0 web server, https://saves.mbi.ucla.edu/, which includes ((Electronic Rapid Response Audit Tool) ERRAT, verify 3D, and PROCHECK modules. The Ramachandran plot has been extensively used to validate the given protein structure in terms of amino acid residues found in allowed or disallowed regions [11]. The final protein structure model was saved in PDBQT format for further analysis.

Drug Profile Evaluation

All 382 Phytoecdysteroids were screened through ProTox-II web server and only those which showed one toxicity were further considered. Only 45 compounds passed this criteria and were used in further calculations.

All 45 Phytoecdysteroids were further evaluated for their pharmacokinetic and pharmacodynamics properties. Various web servers like Swiss ADME and ADMETlab 2.0 were used to estimate several features related to absorption, distribution, metabolism, and excretion (ADME), which are the four major parameters influencing drug pharmacological activity and performance [12–13]. Canonical smiles of the compounds were used as input in the SwissADME server to predict the ADME based on the physicochemical properties, lipophilicity, pharmacokinetics, water solubility, drug-likeness properties, and medicinal properties.

Molecular Docking Studies

Molecular docking studies were performed after structure validation of the homology model. AutoDockTools v1.5.7, which was utilized to generate processed data in pdbqt format for receptors and ligands [14]. AutoDock vina program used for molecular docking [15]. The configuration file was created by defining a grid box of center dimensions X= 19.973, Y= -15.886, Z= 26.742 with sizes X=60, Y=60, and Z=60. This grid box was large enough to accommodate

all the taken ligands. The main objective of the docking was to determine the binding affinities values and bond conformations towards receptors. The docking outputs were saved in log files and out files, which contained the affinity score and docked conformations of each ligand. The root mean square deviation (RMSD) was calculated by using a PyMOL, and it should be less than 3Å to validate the mathematical protocol [16]. The pose with the lowest binding affinity (kcal/mol) was taken and used for further analysis.

Cancer Inhibition Prediction

The pdCSM-cancer server is an anticancer bioactivity prediction platform that is the most comprehensive one developed so far [17].

Server-Based RMSF Analysis

A 10 ns molecular dynamics simulation was conducted separately for both the complex and the protein alone from the CABS-flex server[18]. The root-mean-square fluctuation (RMSF) calculations were performed using an online web server. The root-mean-square-fluctuation (RMSF) of a structure is the time average of the RMSD. It is calculated according to the below equation, where Xi is the coordinates of particle i, and ⟨xi⟩ is the ensemble average position of i.

$$\text{RMSF} = \sqrt{\frac{1}{N}\sum_j^N (x_{i(j)} - \langle x_i \rangle)^2}$$

Where, *xi*(*j*) denotes the position (coordinates) of the *i*-th Cα atom in the structure of the *j*-th model and ⟨*xi*⟩ denotes the averaged position of the *i*-th Cα atom in all models obtained by this method[19].

Results and Discussion

Target Structure Validation

Before performing molecular docking, proteins were prepared and the 3D structures were validated for their correctness by using the SAVES 6.0 server. The 3D structure of proteins PDB ID; 7VKO, 3ZBF, and 3VHK had verified scores of 81.29%, 85.14%, and 79%, respectively, and the ERRAT of the proteins were found to be 96.62, 88.08, and 89.38 respectively. To identify the active sites of proteins, the deposited protein-ligand interactions are available on RCSB. Additionally, utilizing active site prediction servers can be beneficial in pinpointing key regions within the protein structure. Furthermore, as the RMSD is less than 3Å, molecular docking can be carried out. The Ramachandran plot of 7VKO protein was retrieved via the PROCHECK module on the SAVES server. About 92.1% of the amino acid residues were found in the most favored regions, while approximately 7.5% of the residues were present in the additional allowed region. Around 0.4% of residues were located in the generously allowed region, and there were no residues found in the disallowed region. Also, for the 3ZBF protein, 93.4% of residues were found in the most favored region, and 6.2% and 0.4% of residues were in additional allowed regions and generously allowed regions, respectively. At the same time, there was no residue found in the disallowed region. Similarly, for 3VHK protein, 89.2% of residues were found in the most favored region, and 10.2%, and 0.6% residues were in the additional allowed region and generously allowed region, respectively, while there were no residues were found in the disallowed region.For all three receptors, none of the amino acid residues were found in the disallowed regions, and most of the residues were located in the favored region. This suggests that the receptors are of good quality.

Homology Modelling of Protein

Homology modeling is a computational method used to predict the 3D structure of a protein based on its amino acid sequence [20]. The primary sequence of proteins was downloaded from RCSB in fasta format, and the obtained sequence was submitted to the Swiss modeling web server for the prediction of models with a better 3D structure of the protein. The protein with template 7vko.1.A was created and showed the sequence identity of 99% with the GMQE and QMEAN value 0.88 and 0.87±0.05 respectively. For 3ZBF, it has a 100% sequence

identity with template 3zbf.1.A was created. GMQE and QMEAN values of 0.85, and 0.85±0.05 respectively. Similarly, 3VHK showed 100% sequence identity, having a GMQE and QMEAN value of 0.83 and 0.76±0.05 respectively. All the missing amino residues were fulfilled, and the protein models were used for further docking.

Molecular Docking Analysis

A molecular docking procedure was conducted on 45 phytoecdysteroids, and their 2D structure, native ligands, and reference drugs to compare and examine their binding affinities and interactions with the chosen target by using Auto Dock Vina. The binding affinity scores of the selected phytoecdysteroids, native compounds, and reference drugs with PDB ID: 7VKO, 3ZBF, and 3VHK are listed below (**Table 1**). Among 45 phytoecdysteroids, 3 compounds showed higher binding affinities compared to native ligands (-8.9 kcal/mol) in the case of protein 7VKO. Similarly, for 3ZBF, only seven compounds showed better binding affinities than native ligands (-8.4 kcal/mol). Also, for 3VHK, only five compounds showed higher binding affinities than native ligands (-9.0 kcal/mol). PES10 and PES36 showed higher binding affinities, -9.1 and -9.0 kcal/mol respectively, with 7VKO protein. Similarly, for the 3ZBF receptor, PES40 and PES33 showed better binding affinities of -9.2 and -8.8 kcal/mol, respectively. Also, for 3VHK receptors PES25 and PES36 showed better binding affinities of -9.3 and -9.2 kcal/mol respectively. Meanwhile, for the reference drug (Gefitinib), the binding affinity was found to be -7.0 kcal/mol.

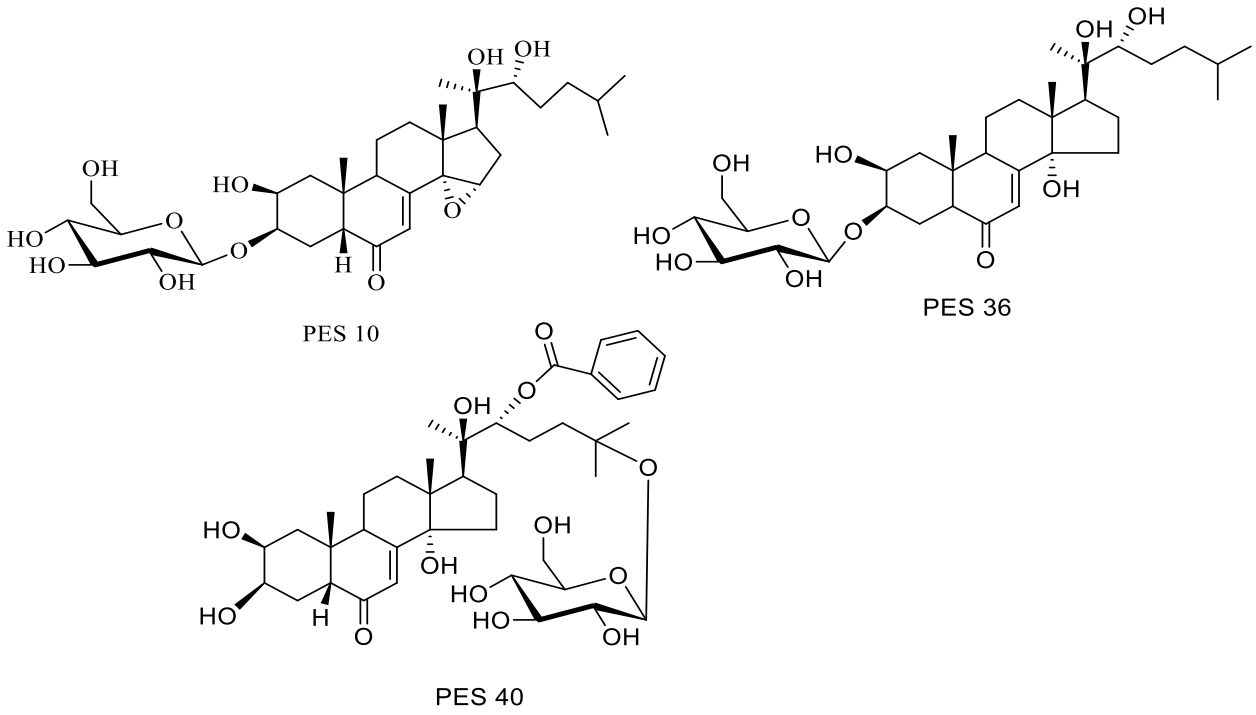

Fig. 1. Molecular structure of top compounds (based on binding affinity)

Table 1: Binding affinities of ligands with the receptor TrkA (PDB ID: 7VKO), ROS1 (PDB ID: 3ZBF) & VEGFR2 (PDB ID: 3VHK)

S.N	Code	Molecular Formula	Binding Affinity (kcal/mol) of ligands with receptors		
			TrkA (PDB ID: 7VKO)	ROS1 (PDB ID: 3VHK)	VEGFR2 (PDB ID: 3ZBF)
1	PES10	$C_{33}H_{52}O_{11}$	**-9.1**	-9.0	-9.0
2	PES36	$C_{33}H_{54}O_{11}$	-9.0	**-9.4**	-9.1
3	PES40	$C_{40}H_{60}O_{13}$	-8.7	-8.8	**-9.2**
4	PES28	$C_{42}H_{62}O_{14}$	-9.0	-8.5	-9.0
5	PES14	$C_{33}H_{56}O_{11}$	-8.9	-8.5	-9.1
6	PES17	$C_{29}H_{46}O_{7}$	-8.9	-8.4	-9.0
7	PES20	$C_{33}H_{56}O_{11}$	-8.9	-8.4	-8.9
8	PES1	$C_{33}H_{56}O_{10}$	-8.8	-8.2	-8.9
9	PES9	$C_{35}H_{58}O_{13}$	-8.8	-8.2	-8.8
10	PES41	$C_{33}H_{56}O_{12}$	-8.8	-8.1	-8.8
11	PES31	$C_{28}H_{16}O_{7}$	-8.6	-8.0	-8.8
12	PES26	$C_{33}H_{56}O_{13}$	-8.5	-7.8	-8.8
13	PES30	$C_{33}H_{54}O_{11}$	-8.5	-7.8	-8.7
14	PES34	$C_{33}H_{56}O_{13}$	-8.5	-7.8	-8.7
15	PES37	$C_{33}H_{56}O_{12}$	-8.5	-7.7	-8.7
16	PES43	$C_{28}H_{16}O_{7}$	-8.5	-7.7	-8.7
17	PES4	$C_{33}H_{54}O_{10}$	-8.4	-7.7	-8.7
18	PES18	$C_{33}H_{56}O_{14}$	-8.4	-7.7	-8.7
19	PES21	$C_{33}H_{56}O_{12}$	-8.4	-7.7	-8.7
20	PES22	$C_{33}H_{56}O_{11}$	-8.4	-7.7	-8.6
21	PES29	$C_{43}H_{61}O_{14}$	-8.4	-7.7	-8.6
22	PES8	$C_{33}H_{56}O_{12}$	-8.3	-7.7	-8.6
23	PES19	$C_{33}H_{56}O_{11}$	-8.3	-7.6	-8.6
24	PES33	$C_{33}H_{52}O_{11}$	-8.3	-7.6	-8.6
25	PES24	$C_{33}H_{54}O_{12}$	-8.3	-7.6	-8.6
26	PES35	$C_{33}H_{54}O_{13}$	-8.3	-7.6	-8.6
27	PES39	$C_{33}H_{54}O_{10}$	-8.3	-7.6	-8.6
28	PES16	$C_{33}H_{56}O_{10}$	-8.2	-7.6	-8.5
29	PES27	$C_{33}H_{56}O_{10}$	-8.2	-7.5	-8.5
30	PES3	$C_{28}H_{46}O_{8}$	-8.1	-7.5	-8.5
31	PES6	$C_{34}H_{58}O_{12}$	-8.1	-7.5	-8.4
32	PES12	$C_{33}H_{54}O_{10}$	-8.1	-7.5	-8.4
33	PES24	$C_{33}H_{54}O_{12}$	-8.1	-7.5	-8.4
34	PES32	$C_{33}H_{56}O_{10}$	-8.1	-7.5	-8.4
35	PES2	$C_{33}H_{56}O_{9}$	-8.0	-7.4	-8.4
36	PES13	$C_{33}H_{54}O_{11}$	-8.0	-7.4	-8.4

37	PES23	$C_{33}H_{54}O_{11}$	-8.0	-7.4	-8.3
38	PES38	$C_{33}H_{56}O_{13}$	-8.0	-7.4	-8.3
39	PES25	$C_{34}H_{54}O_{13}$	-8.0	-7.4	-8.3
40	PES44	$C_{28}H_{46}O_7$	-7.9	-7.3	-8.3
41	PES45	$C_{28}H_{46}O_7$	-7.9	-7.3	-8.2
42	PES5	$C_{35}H_{58}O_{12}$	-7.8	-7.3	-8.2
43	PES11	$C_{33}H_{56}O_{11}$	-7.8	-7.2	-8.1
44	PES7	$C_{33}H_{56}O_{11}$	-7.5	-7.0	-7.9
45	PES15	$C_{35}H_{56}O_{14}$	-7.4	-7.0	-7.9
46	PES42	$C_{28}H_{48}O_5$	-7.4	-6.9	-7.8
47	NL1	$C_{18}H_{18}FN_5O_2$	-8.9	-8.4	-9.0
48	RD	$C_{22}H_{24}ClFN_{43}$	-7.0	-7.0	-7.0

The blue-colored region illustrates the hydrophilic area, resulting from the higher number of electronegative atoms at the surface, while the brown color region signifies the hydrophobic area, characterized by a reduced presence of electronegative atoms (**Fig. 2b, 3b, and 4b**). Additionally, some of the unfavorable bumps (due to the presence of steric hindrance, solvent effects, electrostatic repulsion, and incompatible geometry) have no significant impact on enzyme activity due to the abundance of stabilizing bonding interactions [21]

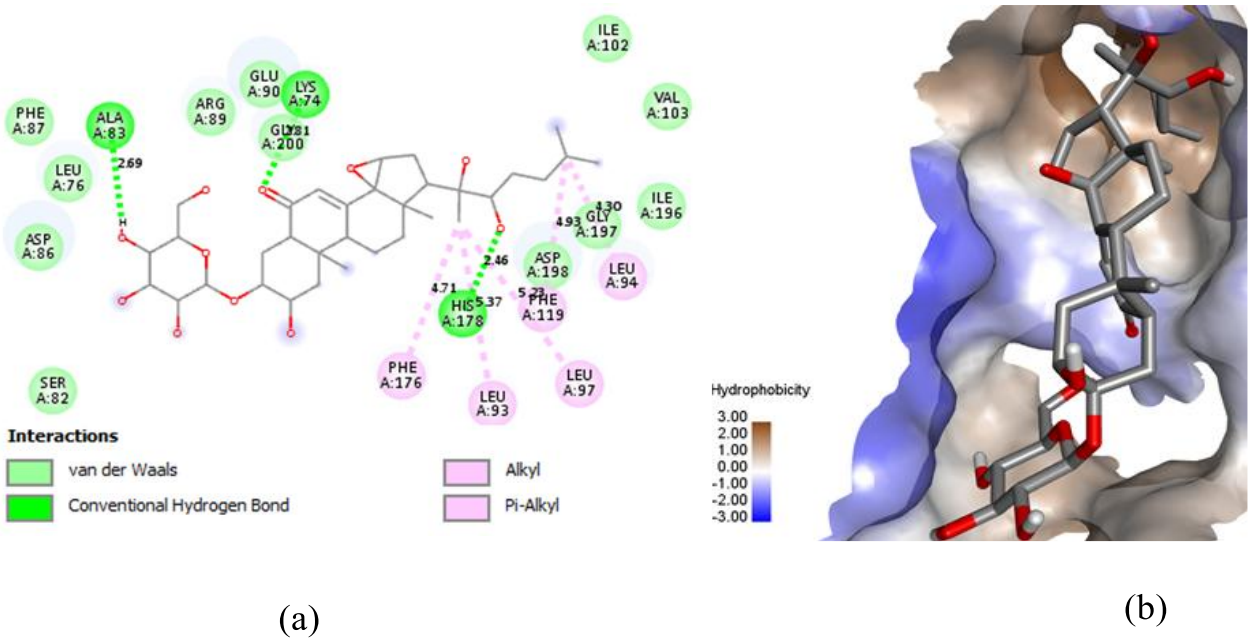

Fig. 2. (a) 2D projection of ligand and active side residues in 7VKO-PES10 adduct; (b) Docking pose of ligand (PES10) in a cavity with hydrophobic surface 7VKO

The lead molecule PES10 has formed hydrogen bonds with the residues HIS178 (2.46), LYS74 (2.81), and ALA83 (2.69). It also formed alkyl and Pi alkyl bonds with the amino acid residues LEU94, LEU97, PHE119, LEU93, and PHE176. Similarly, PES10 established van der Waals bonds with residues PHE87, LEU76, ASP86, SER82, ARG89, GLU90, SER82, ILE102, and VAL103. PES10 was slightly better than the reference drug and native ligand in terms of the number of hydrogen bonds (**Fig. 2a**). This study was supported by a previously reported

article [22].

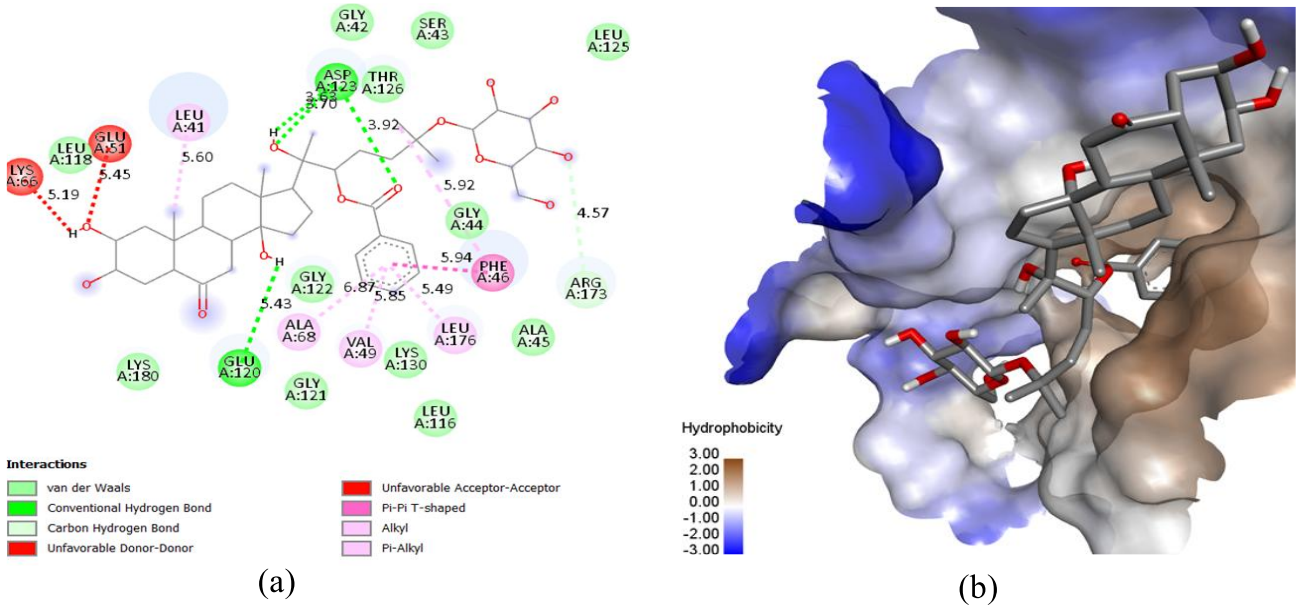

Fig. 3. (a) 2D projection of ligand and active site residues in 3ZBF-PES40 adduct; (b) Docking pose of ligand in the cavity with hydrophobic surface 3ZBF and PES40.

In **Fig. 3(a)**, the leading molecule PES40 was found to show conventional Hydrogen bonding with residues ASP123 (3.63). It also formed alkyl and Pi alkyl and Pi-Pi-T shaped bonds with the residues LEU41, ALA68, VAL49, LEU176, and PHE46. Adduct established van der Waals bonds with residues GLY42, SER43, THR126, LEU125, ALA45, LEU116, LEU118, and GLY121. The results from protein (3ZBF) and Apioside show that there are hydrogen bonds in the amino acids GLU116, ASP123, ARG173, AND GLU120[23].

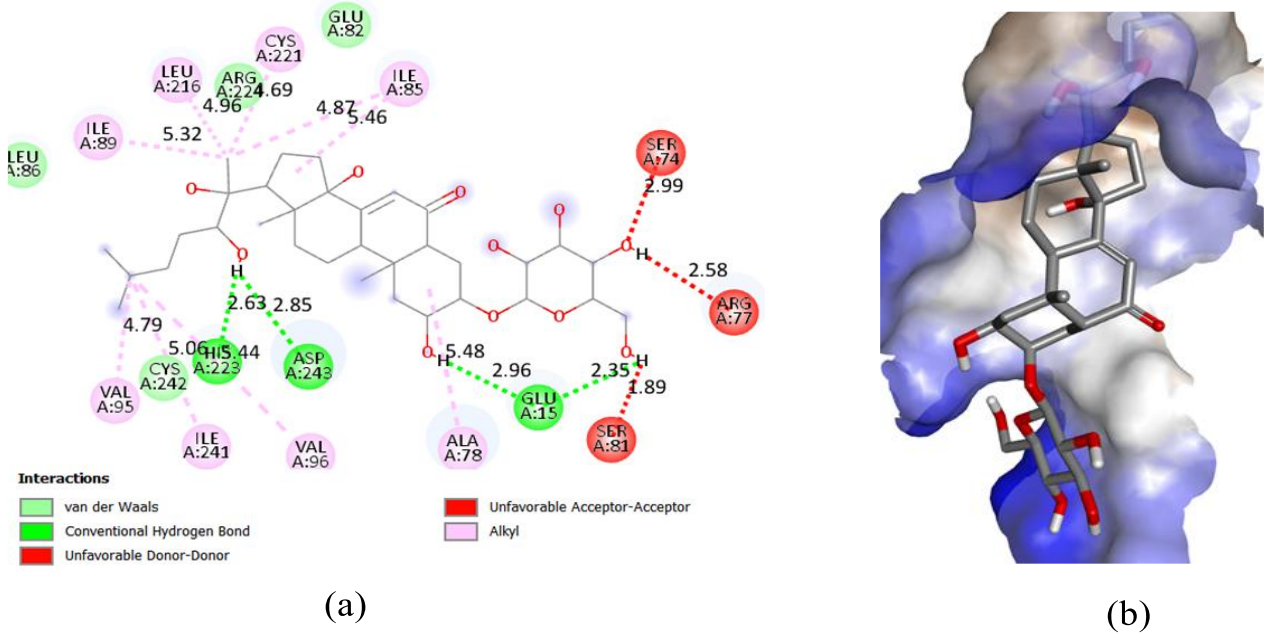

Fig. 4. (a) 2D projection of ligand and active site residues in 3VHK-PES36 adduct; (b) Docking pose of ligand in the cavity with hydrophobic surface 3VHK and PES36.

Fig. 4(a), Adduct shows conventional Hydrogen bonding with residues GLU15 (2.35), HIS223 (2.63), and ASP243 (2.85). It also formed alkyl bonds with the residues ALA78, ILE89, VAL95, VAL96, LEU216, and ILE241. Compound established Vander waals bonds with residues GLU82, ARG224, LEU86, and CYS242. The nearest amino acid residues within 4 Å are GLU15, SER81, ARG77, SER74, GLU12, CYS14, ARG224, HIS223, and ILE222.

ADMET Analysis

It was determined that the inhibitor's antagonistic action to an enzyme or protein receptor does not guarantee the inhibitor's effectiveness as a potential drug [24]. Hence, analyzing ADMET (absorption, distribution, metabolism, excretion, and toxicity) and drug-analysis is a crucial step in drug discovery, as it helps to make an informed decision about the suitability of drugs for a biological system. In addition, most unsuccessful medicines in the clinical phase of research are frequently caused by poor ADME properties and more toxicity effects on the biological system [25].

Following a successful docking-based virtual screening process, the top-performing ligands identified were molecule PES10, PES36, and PES40, with high binding affinity scores with three receptors, which are known anticancer targets with the PDB IDs 7VKO, 3ZBF, and 3VHK, made them ideal candidates for ADME analysis. Upon further examination, PE10, PES36, and PES40 with a synthetic accessibility score of 8.23, 7.89, and 7.85 a predicted bioavailability score of 0.17 for all top hit candidates, low level of GI absorption but no BBB permeation as presented in **table 2**. Synthetic accessibility refers to the ease with which a chemical compound can be synthesized or produced through chemical reactions in a laboratory setting [26]. Bioavailability score refers to a numerical or qualitative measure that assesses the extent and rate at which a substance, typically a drug or a nutrient, is absorbed and becomes available for use or storage in the body [27].

Table 2: Pharmacokinetic properties of hit candidates

S. N	Representative name	GI absorption	BBB Permeant	p-gp substrate	CYP1A2 inhibitor	Log K_p
1	PES10	Low	No	No	No	-9.91
2	PES36	Low	No	No	No	-9.67
3	PES40	Low	No	No	No	-8.93
4	NL1	High	No	Yes	No	-6.98
5	NL2	High	No	Yes	Yes	-6.43
6	NL3	High	Yes	No	Yes	-5.96
7	RD	High	Yes	No	No	-6.11

All the hit candidates except PES25 show a high level of GI absorption, no BBB permeant, and no p-gp substrate however PES25 shows a High GI absorption. Reference drugs including all native ligands show high GI absorption but NL1 and NL2 show no BBB permeant as shown in **Table 2**. So, the hit phytoecdysteroids could be the better candidates for lung cancer inhibitors.

Table 3. Toxicity of hit candidates with reference drug

S.N.	Representative name	Hepatotoxicity	Carcinogenicity	Immunotoxicity	Mutagenicity	Cytotoxicity
1	PES10	Inactive	Inactive	Active	Inactive	Inactive
4	PES36	Inactive	Inactive	Active	Inactive	Inactive
5	PES40	Inactive	Inactive	Active	Inactive	Inactive
6	NL1	Active	Inactive	Active	Inactive	Inactive
7	NL2	Inactive	Active	Active	Inactive	Inactive
8	NL3	Inactive	Inactive	Inactive	Inactive	Inactive
9	RD	Active	Inactive	Active	Inactive	Inactive

All the hit candidates, native ligands, and reference drugs show at least one toxicity except NL3. PES10, PES25, PES33, PES36, and PES40 show immunotoxicity active and other parameters are inactive, but for reference drug and NL1, both hepatotoxicity and immunotoxicity are active which was enlisted in **Table 3**.

Cancer Inhibition Prediction by pdCSM

The anticancer inhibitory activity of small ligands can be studied from pdCSM which predicts these ligands' anticancer bioactivity against many cancer cell lines.

Table 4. pdCSM different parameters of hit candidates, native ligands, and reference drug

S.N.	Representation	Activity	Breast MDA_MB_468	CNS SF_539	Colon HCT_116	Lk P388	Mn MDA_MB_435	NS NCI_H522	Small DMS_273
1	PES10	Inactive	6.663	5.026	5.34	6.354	5.901	5.261	4.274
4	PES36	Inactive	6.749	4.731	4.502	6.446	5.331	4.953	4.391
5	PES40	Inactive	6.829	5.257	5.335	5.894	5.26	5.635	6.259
6	NL1	Inactive	5.436	4.552	4.452	5.366	5.566	4.564	4.421
7	NL2	Active	5.484	5.042	5.268	5.541	5.309	5.152	5.264
8	NL3	Inactive	5.064	4.484	4.404	4.884	4.723	4.511	4.168
9	RD	Inactive	5.734	4.958	5.369	5.344	5.108	5.248	5.632

Ac: Anticancer, Lk: Leukemia, Mn: Melanoma, NS: Nonsmall

The pdCSM server shows overall inactivity of hit candidates except native ligand NL2, they are active towards specific cancer cell lines since values greater than 5 indicate activity towards specific cell lines. PES 10 was active against MDA_MB_468, HCT_116, SF_539, P388, MDA_MB_435, and NCI_H522 cancer cell lines. PES 25 are active against MDA_MB_468, SF_539, P388, MDA_MB_435, and NCI_H522 cell lines. PES36 were active against only MDA_MB_468, SF_539, P388, and MDA_MB_435 cell lines. PES33 was active for all cell lines except HCT_116 and PES40 was active against all cell lines. Native ligand (NL1) was active against MDA_MB_468, P388, and MDA_MB_435 cell lines.NL2 was active for all cell lines. Similarly, NL3 was active against only the MDA_MB_468 cell line and the reference drug was active against all cell lines except the SF_539 line as shown in **Table 4**.

RMSF of Adducts

To further validate the results obtained from

our molecular docking analysis, there was the evaluation of the stability of four different adducts (PES10, PES36, PES33, PES40, PES25) using a server-based MD simulation and assessed the MD simulation results by analyzing the RMSF values. RMSF values indicate the degree of fluctuations and flexibility of the protein during the simulation. Lower RMSF values indicate minimal conformational changes, which means that the protein is more stable. Conversely, higher RMSF values suggest greater flexibility. It was observed that the stability of the complexes was superior to that of the protein alone. The given plots demonstrated that there were more positive values than negative ones, indicating that the protein was less fluctuated when it was bound to the ligand, and the mathematical form for RMSF is given by,

ΔRMSF= RMSF of amino acid in a protein in holo form – RMSF of amino acid in a protein in the apo form

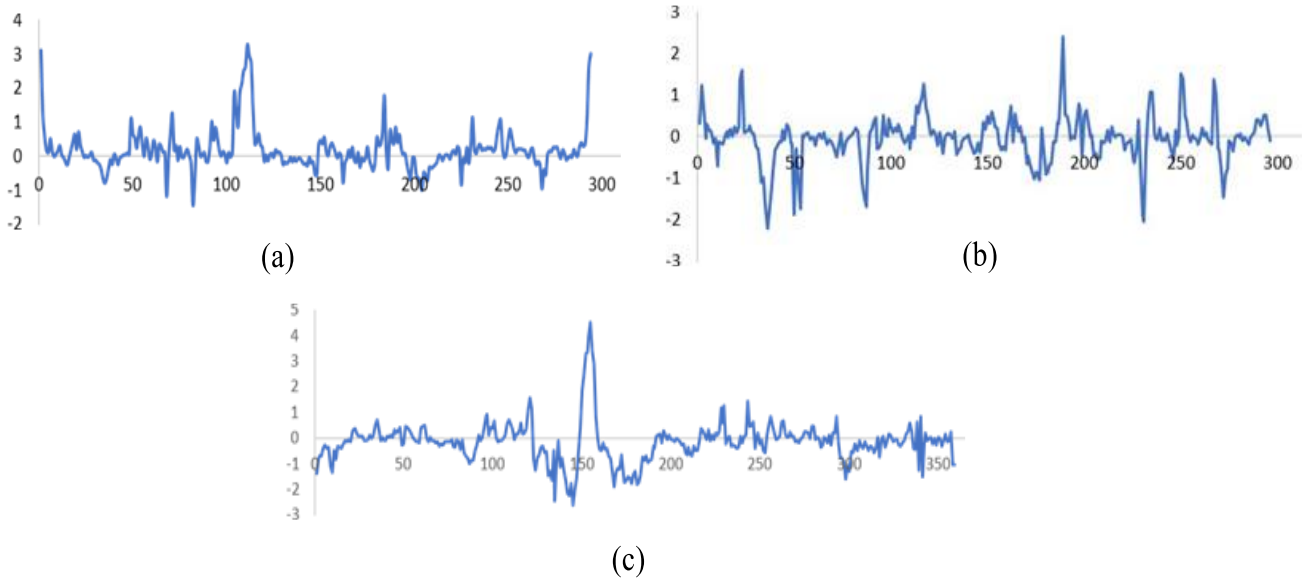

Fig 5. RMSF difference plot of (a) VKO with PES10; (b) 3ZBF with PES40; (c) VHK with PES36

The RMSF determines the flexibility of amino acid residues. It is critical for monitoring local protein changes because it allows calculating the average change detected over many atoms to determine the displacement compared to the reference structure [28]. The MD simulations revealed that the binding pocket was relatively stable, as evidenced by the RMSF values obtained for each residue surrounding the ligand in the protein complex [29] as presented in **Fig. 5.** The difference in root mean square fluctuations between the complex and protein for each residue was determined in which **Fig. 5 (a)** residues exhibit positive peaks (83) in their ΔRMSF, while only a few exhibit negative peaks (-28) leading the sum of the ΔRMSF of each residue is overall positive, indicating that the complex is stable and has minimal fluctuations. Most residues exhibit negative peaks (-62.108) in their ΔRMSF, while only a few exhibit positive peaks (46.216) in **Fig. 5 (b)**. This implies that the sum of the ΔRMSF of each residue is overall negative, indicating that the complex is unstable and has maximum fluctuations. The same is the result for **Fig. 5 (c)**, which exhibit negative peaks (-120.084) in their ΔRMSF, while only a few exhibit positive peaks (66.625). This implies that the sum of the ΔRMSF of each residue is overall negative, indicating that the complex is unstable and has maximum fluctuations [28].

Conclusions

The potential of phytoectosteroids to inhibit promising target compounds has exhibited a promising bioavailability score while also

demonstrating no apparent indications of carcinogenesis, mutagenesis, hepatotoxicity, and cytotoxicity. When compared to the reference drug, the binding affinity score was better and also showed less toxicity of hit candidates with all three proteins. Molecular dynamics simulations were used to investigate the stability of the top phytoecdysteroids with the best docking results. So, *in silico* findings indicate that phytoecdysteroids have the potential to inhibit TrkA, ROS1, and VEGFR could be explored further as a possible anticancer agent. Based on these findings, additional *In vitro* and *In vivo* clinical trials are required, as well as further simulations. Therefore, this research work suggests conducting inhibition assays to assess the anticancer properties of the hit compound.

Acknowledgment

The authors are grateful to Dr. Subin Adhikari for his valuable input while conducting this work

Author's Contribution Statement

Bishnu Adhikari: Methodology, Investigation, Formal analysis Data curation, **Ashish Phuyal:** Methodology, Investigation, Formal analysis, Data curation, Writing-original draft preparation, Writing-review and editing. **Anuraj Phunyal:** Investigation, Formal analysis, Data curation, Writing-original draft preparation. **Nabin Upadhyaya:** Formal analysis, editing, **Amar Waiba:** Methodology, Investigation, formal analysis **Achyut Adhikari**: Conceptualization, Resources, Funding acquisition, Writing-review and editing, supervision.

Conflict of Interest

The authors declare that they have no conflicts of interest.

Data Availability Statement

The data supporting this study's findings are available from the corresponding authors upon reasonable request.

References

1. M. S. Chandraprasad, A. Dey, & M. K. Swamy, Introduction to cancer and treatment approaches, *Paclitaxel*, 2022, 1–27. (DOI: https://doi.org/10.1016/B978-0-323-90951-8.00010-2)
2. B. Koul, Types of Cancer, *Herbs Cancer Treat*, 2019, 53–150. (DOI: https://doi.org/10.1007/978-981-32-9147-8_2)
3. W. Zhang, W. Tian, Y. Wang, X. Jin, H. Guo, Y. Wang, Y. Tang, & X. Yao, Explore the mechanism and substance basis of Mahuang FuziXixin Decoction for the treatment of lung cancer based on network pharmacology and molecular docking, *Computers in Biology and Medicine*, 2022, 151, 106293. (DOI: https://doi.org/10.1016/j.compbiomed.2022.106293)
4. C. Zappa & S. A. Mousa, Non-small cell lung cancer: current treatment and future advances, *Translational Lung Cancer Research*, 2016, 5, 288–300. (DOI: https://doi.org/10.21037/tlcr.2016.06.07)
5. N. Das, S. K. Mishra, A. Bishayee, E. S. Ali, & A. Bishayee, The phytochemical, biological, and medicinal attributes of phytoecdysteroids: An updated review, *Acta Pharmaceutica Sinica B*, 2021, 11, 1740–1766. (DOI: https://doi.org/10.1016/j.apsb.2020.10.012)
6. N. Sood, S. Chaudhary, T. Pardeshi, S. Mujawar, K. B. Deshmukh, S. A. Sheikh, & P. Sharma, In-silico study of small cell lung cancer based on protein structure and function: A new approach to mimic biological system, *Journal of Advanced Pharmaceutical Technology & Research*, 2015, 6, 125–129. (DOI: https://doi.org/10.4103/2231-4040.161513)
7. M. D. Hanwell, D. E. Curtis, D. C. Lonie, T. Vandermeersch, E. Zurek, & G. R. Hutchison, Avogadro: an advanced semantic chemical editor, visualization, and analysis platform. *Journal of Cheminformatics*, 2012, 4, 17. (DOI: https://doi.org/10.1186/1758-2946-4-17)
8. L. L. C. Schrodinger, The PyMOL molecular graphics system, *Version*, 2015, 1, 8.

9. M. Biasini, S. Bienert, A. Waterhouse, K. Arnold, G. Studer, T. Schmidt, F. Kiefer, T. G. Cassarino, M. Bertoni, L. Bordoli, & T. Schwede, SWISS-MODEL: modelling protein tertiary and quaternary structure using evolutionary information. *Nucleic Acids Research*, 2014, 42, W252–W258. (DOI: https://doi.org/10.1093/nar/gku340)
10. A. H. A. Maghrabi & L. J. McGuffin, ModFOLD6: an accurate web server for the global and local quality estimation of 3D protein models. *Nucleic Acids Research*, 2017, 45, W416–W421. (DOI: https://doi.org/10.1093/nar/gkx332)
11. S. A. Hollingsworth & P. A. Karplus, A fresh look at the Ramachandran plot and the occurrence of standard structures in proteins, 2010, 1, 271–283. (DOI: https://doi.org/10.1515/bmc.2010.022)
12. A. Daina, O. Michielin, & V. Zoete, SwissADME: a free web tool to evaluate pharmacokinetics, drug-likeness and medicinal chemistry friendliness of small molecules, *Scientific Reports*, 2017, 7, 42717. (DOI:https://doi.org/10.1038/srep42717)
13. G. Xiong, Z. Wu, J. Yi, L. Fu, Z. Yang, C. Hsieh, M. Yin, X. Zeng, C. Wu, A. Lu, X. Chen, T. Hou, & D. Cao, ADMETlab 2.0: an integrated online platform for accurate and comprehensive predictions of ADMET properties, *Nucleic Acids Research*, 2021, 49, W5–W14. (DOI:https://doi.org/10.1093/nar/gkab255)
14. G. M. Morris, R. Huey, W. Lindstrom, M. F. Sanner, R. K. Belew, D. S. Goodsell, & A. J. Olson, AutoDock4 and AutoDockTools4: Automated docking with selective receptor flexibility, *Journal of Computational Chemistry*, 2009 ,30, 2785–2791. (DOI: https://doi.org/10.1002/jcc.21256)
15. O. Trott & A. J. Olson, AutoDock Vina: Improving the speed and accuracy of docking with a new scoring function, efficient optimization, and multithreading, *Journal of Computational Chemistry*, 2010, 31, 455–461. (DOI: https://doi.org/10.1002/jcc.21334)
16. A. Phunyal, A. Adhikari, & J. A. Subin, *In silico* exploration of potent flavonoids for dengue therapeutics, *PLOS ONE*, 2024, 19 e0301747. (DOI: https://doi.org/10.1371/journal.pone.0301747)
17. R. Al-Jarf, A. G. C. De Sá, D. E. V. Pires, & D. B. Ascher, pdCSM-cancer: Using Graph-Based Signatures to Identify Small Molecules with Anticancer Properties, *Journal of Chemical Information and Modeling*, 2021, 61, 3314–3322. (DOI: https://doi.org/10.1021/acs.jcim.1c00168)
18. A. Kuriata, A. M. Gierut, T. Oleniecki, M. P. Ciemny, A. Kolinski, M. Kurcinski, & S. Kmiecik, CABS-flex 2.0: a web server for fast simulations of flexibility of protein structures, *Nucleic Acids Research*, 2018, 46, W338–W343. (DOI: https://doi.org/10.1093/nar/gky356)
19. A. Badaczewska-Dawid, A. Kolinski, & S. Kmiecik, Protocols for fast simulations of protein structure flexibility using CABS-flex and SURPASS, 2019 694026. (DOI: https://doi.org/10.1101/694026)
20. M. T. Muhammed & E. Aki-Yalcin, Homology modeling in drug discovery: Overview, current applications, and future perspectives, *Chemical Biology & Drug Design*, 2019, 93, 12–20. (DOI: https://doi.org/10.1111/cbdd.13388)
21. D. Karki, A. Phunyal, T. R. Lamichhane, A. Rayamajhi, A. Sapkota, H. Nyaupane, S. Shrestha, & A. Adhikari, Chemical profiling, in-vitro and *in silico* α-glucosidase inhibition, antioxidant and antibacterial activities of Hypotrachyna cirrhata (Fr.) Hale ex Sipman, *All Life*, 2024 , 17, 2424894. (Doi: https://doi.org/10.1080/26895293.2024.2424894)
22. C. Kirubhanand, J. Merciline Leonora, S. Anitha, R. Sangeetha, K. T. Nachammai, K. Langeswaran, & S. Gowtham Kumar, Targeting potential receptor molecules in non-small cell lung cancer (NSCLC) using *in silico* approaches, *Frontiers in Molecular Biosciences*, 2023, 10, 1124563. (DOI: https://doi.org/10.3389/fmolb.2023.1124563)
23. P. Santoso, K. A. Adrianta, A. A. C. Wibawa, & I. W. S. A. Gunawan, Molecular docking activity of peristrophe bivalvis on non small cell lung cancer,

Jurnal Aisyah : Jurnal Ilmu Kesehatan, (2023), 8,. (DOI: https://doi.org/10.30604/jika.v8i2.1935)

24. A. B. Umar, A. Uzairu, G. A. Shallangwa, & S. Uba, Design of potential anti-melanoma agents against SK-MEL-5 cell line using QSAR modeling and molecular docking methods, *SN Applied Sciences*, 2020, 2, 815. (DOI: https://doi.org/10.1007/s42452-020-2620-8)
25. S. Attique, M. Hassan, M. Usman, R. Atif, S. Mahboob, K. Al-Ghanim, M. Bilal, & M. Nawaz, A Molecular Docking Approach to Evaluate the Pharmacological Properties of Natural and Synthetic Treatment Candidates for Use against Hypertension, *International Journal of Environmental Research and Public Health*, 2019, 16, 923. (DOI: https://doi.org/10.3390/ijerph16060923)
26. P. Ertl & A. Schuffenhauer, Estimation of synthetic accessibility score of drug-like molecules based on molecular complexity and fragment contributions, *Journal of Cheminformatics*, 2009, 1, 8. (DOI: https://doi.org/10.1186/1758-2946-1-8)
27. Y. C. Martin, A Bioavailability Score, *Journal of Medicinal Chemistry*, 2005, 48, 3164–3170. (DOI: https://doi.org/10.1021/jm0492002)
28. F. Ahammad, R. Alam, R. Mahmud, S. Akhter, E. K. Talukder, A. M. Tonmoy, S. Fahim, K. Al-Ghamdi, A. Samad, & I. Qadri, Pharmacoinformatics and molecular dynamics simulation-based phytochemical screening of neem plant *(Azadiractha indica)* against human cancer by targeting MCM7 protein, *Briefings in Bioinformatics*, 2021, 22, bbab098. (DOI: https://doi.org/10.1093/bib/bbab098)
29. R. Lal Swagat Shrestha, B. Maharjan, T. Shrestha, B. Prasad Marasini, & J. Adhikari Subin, Geometrical and thermodynamic stability of govaniadine scaffold adducts with dopamine receptor D1, *Results in Chemistry*, 2024, 7, 101363. (doi:https://doi.org/10.1016/j.rechem.2024.101363)